Front. Earth Sci. 2018, 12(3): 521–531
https://doi.org/10.1007/s11707-017-0672-x

RESEARCH ARTICLE

Remote sensing study of wetlands in the Pearl River Delta during 1995—2015 with the support vector machine method

Xiaosong HAN, Jiayi PAN (✉), Adam T. DEVLIN

Institute of Space and Earth Information Science, The Chinese University of Hong Kong, Hong Kong, China

Abstract In recent years, the Pearl River Delta has experienced rapid economic growth which may create a substantial burden to its ecology. In this study, the wetlands of the Pearl River Delta are investigated. Through the use of remote sensing methods, we analyze spatial and temporal variations of wetlands in this area over the past twenty years. The support vector machine (SVM) method is proven to be an effective approach for classifying the wetlands of the Pearl River Delta, and the total classification resolution reaches 94.94% with a Kappa coefficient exceeding 0.94, higher than other comparable analysis methods. Our results show that wetland areas were reduced by 36.9% during the past twenty years. The change detection analysis method shows that there was a 95.58% intertidal zone change to other land-use types, most of which (57.12%) was converted to construction land. In addition, farmland was reduced by 54.89% during the past twenty years, 47.19% of which was changed to construction land use. The inland water area increased 19.02%, but most of this growth (18.77%) was converted from the intertidal zone.

Keywords wetland, Pearl River Delta, support vector machine method, Landsat images

1 Introduction

Wetlands are an important part of the Earth's ecosystem and have rich bio-diversity which can assist in resource conservation for human use (Kristine Butera, 1983). Presently, there is a trend of decreasing wetland areas in many parts of the world. In the US, coastal wetlands lost roughly 33,230 acres from 1998 to 2004 (Dahl, 2006). In France, nearly 67% of wetland regions have disappeared in the past century. Since the 1950s, 84% of swamplands have vanished in England and 57% in Germany, both owing to rapid urbanization (Silva et al., 2007). From 1978 to 2008, the wetland areas of China decreased by about 33%, and economic development caused considerable wetland loss in most eastern provinces (Niu et al., 2012).

Against this backdrop, the question of how to protect the wetlands has become an urgent issue. Evaluating the existing wetlands and understanding their spatial and temporal changes can assist in the implementation of effective measures for wetland protection. The traditional field survey methodology of wetlands is time-consuming and requires substantial inputs of manpower and other resources. As an alternative, remote sensing technology is a useful method to monitor the changing wetlands, especially on a large scale. A number of analysis methods were developed to extract or classify different land surfaces from satellite remote sensing images.

The support vector machine (SVM) method is defined as a supervised model which is combined with learning algorithms to analyze remote sensing data used for classification (Melgani and Bruzzone, 2004). The main aim of SVM is to find the optimal hyperplane which has the maximum margin that can linearly separate the two classes. When the training data are not linearly separable in the input space, SVM can use kernel functions to project the training data to a feature space of a higher dimension, in which the linear separation becomes easier (Vapnik, 1995). The SVM classification method has received more attention in recent years using remote sensing data analysis, especially in land-cover classification (Ceamanos et al., 2010; Wu et al., 2012; Lin et al., 2013; Fan et al., 2014; Zhang et al., 2015; Kamlun et al., 2016; Pretorius et al., 2016). Wu et al. (2012) used SVM to simulate the distribution of land cover in Beijing, and the results indicate that the SVM model has high classification accuracy and strong generalization ability. Fan et al. (2014) analyzed the land cover of Yi Liang County with the SVM method, and the results show that SVM

Received March 18, 2017; accepted July 21, 2017

E-mail: panj@cuhk.edu.hk

classification results are generally better than the Maximum Likelihood classification results, especially in small sample and multi-dimension conditions, with the overall accuracy of the classification results reaching 88.13%. Pretorius et al. (2016) studied the land cover in South Africa, and found that when the study area has many complex land cover types, the SVM method has obvious advantages in dealing with these complex issues.

Ceamanos et al. (2010) focused on performances between an SVM fusion ensemble and a standard SVM classifier. Lin et al. (2013) used a mixed kernel function to improve the accuracy of the classification results. Zhang et al. (2015) compared the different classification results by changing parameter settings and adding training subsets. However, these existing studies mainly focused on the choice of parameter settings for SVM, which is mainly applied to inland areas. There have been few investigations using the SVM method to classify water surface and land-water mixture (including wetlands) in the coastal area. The SVM is a classification method based on statistics, which means that the appropriate definition of the data sources plays an important role in determining the final classification accuracy (Wang et al., 2007). In this study, we employ the SVM method in the coastal region to validate its reliability in classifying wetlands in the coastal areas which have different spectral characteristics and dynamic properties from the inland regions. Based on field investigation and other useful data, we select a large number of reliable training samples in the Pearl River Delta to examine the accuracy of the SVM classification method.

2 Methods

2.1 Study region and data sources

The Pearl River Delta is formed by the downstream alluvial effects of the Xijiang, Beijiang, Dongjiang, and Tanjiang Rivers, as well as many secondary minor streams. The total area of the Pearl River Delta is about 2.79×10^6 acres, including the area of Guangzhou, Foshan, Zhongshan, Zhuhai City, part of Shenzhen City, and Dongguan County, among others, which covers almost all the urbanized regions in Guangdong Province. Accordingly, the wetlands in this area have been greatly affected by human activity.

The Landsat TM/OLI/TIRS (Thematic Mapper/Operational Land Imager/Thermal Infrared Sensor) multi spectral instruments are one of the most effective remote sensing data sources, since they can make observations in the visible, near infrared, infrared, and thermal infrared bands, with a time span from the mid-1980s to present. Table 1 show the Landsat data used (with the resolution of 30 m×30 m) from the Landsat 4-5 and Landsat 8 archives.

Table 1 Time and instrument of Landsat TM/OLI/TIRS images

Image time	Sensor
December 30, 1995	Landsat 4-5 TM
November 01,1997	Landsat 4-5 TM
December 09, 1999	Landsat 4-5 TM
December 30, 2001	Landsat 4-5 TM
December 4, 2003	Landsat 4-5 TM
November 23, 2005	Landsat 4-5 TM
January 29, 2007	Landsat 4-5 TM
November 02, 2009	Landsat 4-5 TM
June 01, 2011	Landsat 4-5 TM
November 29, 2013	Landsat 8 OLI/TIRS
October 18, 2015	Landsat 8 OLI/TIRS

However, there are also some disadvantages in using the Landsat data. Cloud coverage is an important criterion for testing the quality of remote sensing images. Subtropical areas always have many clouds in summer, which hampers the interpretation of remote sensing images, so the Landsat images in this study are mainly taken in winter as the weather is not as cloudy then. Also, the Landsat satellites orbit in a fixed orientation, so in some areas the complete images require splicing together multiple pictures. Figure 1 shows the coverage area of the Landsat images, ranging from 22°41′9″N to 22°57′18″N and 113°28′30″E to 113°45′54″E, with an area of 222,395 acres.

2.2 Image preprocessing

The first step of the experiment is the radiation correction and geometric rectification of the 11 images employed in this study. Because the solution to the atmospheric radiative transfer equation requires numerous measured parameters, the acquisition of these parameters often has many problems. Therefore, this paper adopts the histogram matching method (Liang et al., 2001) of the relative atmospheric correction method for radiation correction. The histogram of TM images in 1995 is used as the reference, and the histograms of other TM/OLI/TIRS images are compared to this calibration image. In terms of the geometric rectification, we use the image registration method to correct the initial TM/OLI/TIRS images. Figure 2 shows the final preprocessing results, which are comparable for the different images, therefore allowing for an accurate determination of trends.

2.3 Sample selection (ROI)

After preprocessing the images, the second step is to determine the classification system of the study area, which we will also define as selecting the region of interest (ROI). The coastal area of the Pearl River estuary is a typical

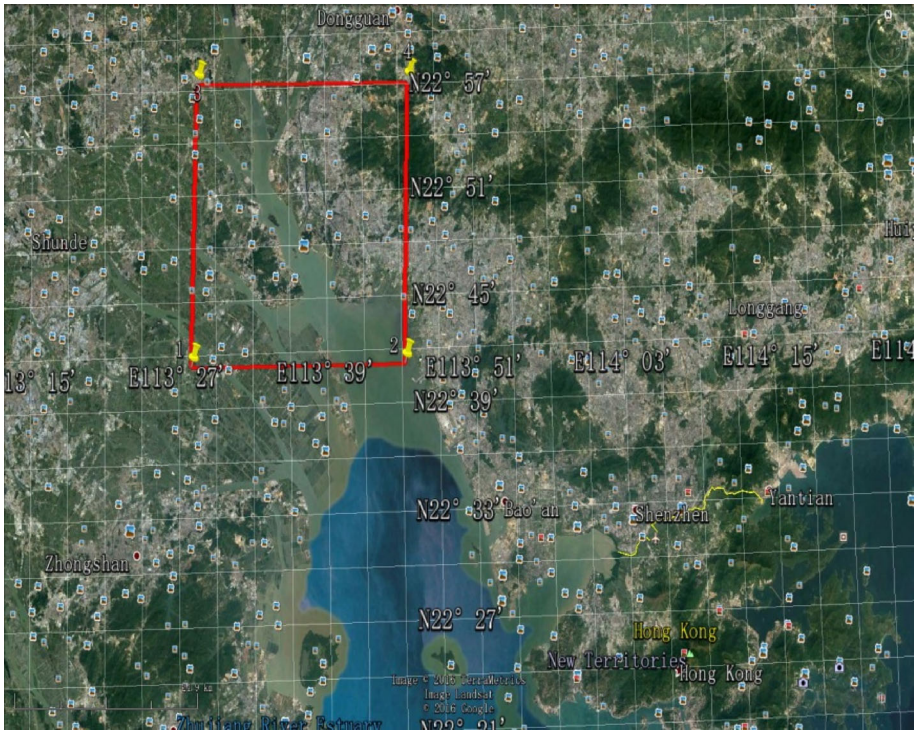

Fig. 1 The study area (red) on a Google map image (June 7, 2015).

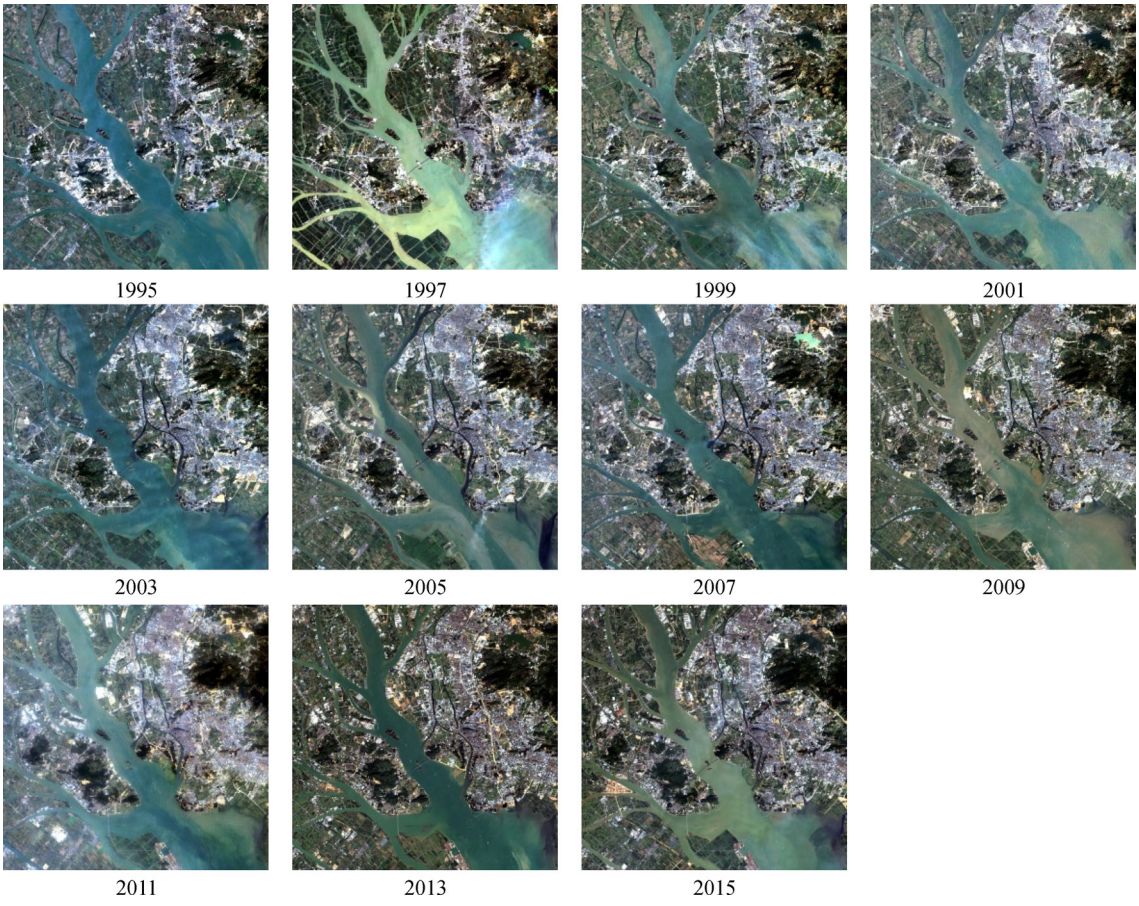

Fig. 2 11 TM/OLI/TIRS images downloaded from USGS after radiation correction and geometric rectification from 1995 to 2015.

estuarine coastal wetland which includes a variety of wetland types.

Using the determinations of previous research (Lin et al., 2013) and the special characteristics of the Pearl River Delta, the ROIs in this paper are determined as follows:

1) Water. This mainly represents the salty water from the ocean.

2) Mountain forest. Since the Ramsar Convention on Wetlands (Li, 2001) does not consider mountainous forested regions part of the wetlands, it has been selected as the second ROI to help us to separate it from the wetlands.

3) Urban areas. The rapid economic development of the Pearl River Delta accelerates the speed of urbanization and may have reduced the area of the wetlands. As this mechanism is the main hypothesis of this study, the selected pixels defined as this ROI comprise the majority of our study region.

In addition to the previous non-wetland ROIs, the wetland regions are divided into three ROI categories:

4) Inland water. This also includes natural wetlands; i.e., permanent rivers, streams, lakes, and shallow water near the ocean. Artificial wetlands containing reservoirs and ponds also are included in this ROI classification.

5) Coastal wetlands. These are mainly composed of the intertidal beach and the inland swamp regions near the rivers and lakes.

6) Farmland. The majority of crops in the Pearl River Delta are paddies, one of nine kinds of artificial wetlands as determined by the Ramsar Convention on Wetlands. Additionally, there are some man-made mangrove forests in this area, which are merged with the paddy ROI for our purposes.

2.4 Classification strategy

2.4.1 Unsupervised classification

Unsupervised classification is the simplest model of remote sensing image classification, which is also defined as clustering classification or point group analysis (Zhao, 2003). The process of unsupervised classification involves clustering based on the spectral characteristics of different objects in remote sensing images. Consequently, the requirements for the knowledge of the research area in the unsupervised classification template are lower compared with other classification models. However, when the unsupervised classification is executed to classify the remote sensing images, it demands that the same object on the ground has a uniform spectrum under the same imaging conditions. Under this situation, the results of the unsupervised classification cannot ensure a high accuracy due to the same object possibly having many spectrums in the same image. Generally, the algorithm of unsupervised classification is to repeat the cycle until the final results are expected when compared with the initial convergence threshold.

2.4.2 Supervised classification

Supervised classification extracts a training sample from the auxiliary information about the study area, which can help us to classify the objects in the remote sensing images. When we have some former knowledge and data about the study area, we can use the supervised classification to add this information into the classification process to improve the final accuracy. As a result, the most important step in the supervised classification is to build a reliable classification template, in which we need to select many training and testing samples to repeat our experiment until the final classification accuracy achieves the expected value. Normally, the minimum distance method and maximum likelihood method are the most commonly used algorithms in the supervised classification. But the algorithm of the support vector machine (SVM) method has specific advantages in classifying the remote sensing images.

2.4.3 Support Vector Machine

Generally, SVMs can be divided into two cases: 1) linearly separable case; 2) linearly non-separable case. The optimal classification functions for these two cases are as follows:

$$f_1(x) = \mathrm{sgn}\left\{\sum_{i=1}^{n} a_i y_i (x_i * x) + b\right\}, \tag{1}$$

$$f_2(x) = \mathrm{sgn}\left\{\sum_{i=1}^{n} a_i y_i K(x_i * x) + b\right\}. \tag{2}$$

The benefits of using the SVM method are: 1) it is specifically aimed at finite samples, whose objective is to obtain the optimal solution under the existing information, not just the optimal value of the sample number (Melgani and Bruzzone, 2004); 2) the algorithm will eventually be transformed into a two-type optimization problem. In theory, the obtained sample will be the most representative of the global solution, and it also avoids the local extreme value problem in the neural network method (Waske and Benediktsson, 2007).

For the SVM parameterization in this study, we choose the radial basis function as the kernel type and the gamma of the kernel function as 0.167. We use a default value of 100 as the penalty parameter and the pyramid level is 0, which means that we use the original resolution to classify the images. The last parameter of the SVM is the classification probability threshold. In this experiment, as all the pixels in the images need to be considered, this value is 0.

2.5 Accuracy evaluation

The accuracy for the classification of remote sensing images is defined as the differences found from comparing the results from the classification template with the actual situation in this area. Therefore, the accuracy evaluation is an important way to ensure the reliability of the experiment. It also can be used as an indicator to reflect different classification models in extracting the same objects from the same remote sensing images. Three indicators (confusion matrix, total classification accuracy, and kappa coefficient) are used to evaluate the classification results.

2.5.1 Confusion matrix

A confusion matrix is used to show the performance of a classification algorithm, also known as an error matrix (Stehman, 1997). The columns and rows of the matrix represent the instances in a predicted class and in an actual class (or vice versa), respectively (Powers, 2011). The confusion matrix is a basic way to describe the comparison results between the results from the support vector machine and the actual condition of the objects on the ground (Wu et al., 2017). Usually through ENVI® post-classification tools, we can get a matrix containing information about the deviation, which also provides us with the necessary data for ENVI® to calculate both the total classification accuracy and the kappa coefficient.

2.5.2 Total classification accuracy

The formula for total classification accuracy calculation uses the total classified samples divided by the properly classified samples. We usually have more than one ROI in our experiments, so it is necessary to consider all correct classified samples when the final accuracy is derived. The equation is as follows:

$$P = \frac{\sum_{k=1}^{n} S_k}{S}, \tag{3}$$

where n is the total ROIs, k represents the different ROI, S_k is the amount of correct classified samples on the diagonal of the matrix, and S is the number of the sample.

2.5.3 Kappa coefficient

Under the situation that the total classification accuracy is limited by the correct classified samples on the diagonal of the matrix, we need a more accurate method to evaluate the result. Cohen (1960) proposed the concept of the kappa coefficient, which synthetizes all the data from the confusion matrix. The kappa coefficient is a measure of the difference between the real consistency and the variation which gives a quantitative evaluation of the classification results. According to previous studies, a kappa coefficient higher than 80% is an adequate classification result (Brennan and Prediger, 1981; Næsset, 1996; Lillesan and Kiefer, 2000).

2.6 Change detection statistics

Change detection statistics are a set of function in ENVI® which offers a straightforward way of measuring the variations between multiple images that stand for the initial state and the final state (Pretorius et al., 2016). After we use the training ROIs to obtain the classifications of the study area, the change detection statistics tool will generate a change table of different ROIs among the study period. From the final table, we can obtain details about the spatial change under different classification indices.

3 Results

After we execute the support vector machine classification model with the ROIs we select on the remote sensing images, the study area can be divided into different types of ground objects, shown in Fig. 3.

In the final classification images, different colors indicate different objects on the ground. According to the former regions of interest (ROI) that we designed as the training samples, the first ROI (water area) is Blue 3; the second (mountain forest region) is Green 3 in the images, and the third ROI (urban areas) is represented by sienna in the final results. Subdivisions of the wetlands are shown including inland water (Blue 1), coastal wetlands (yellow), and farmland (Green 1) which were all generated based on these 11 images. From these figures we can see that there is an obvious trend of urban expansion in the Pearl River Delta. However, these training samples need testing samples to evaluate their accuracy, so the testing ROIs of the raw images with different areas to training samples are selected, and the number of pixels of testing ROIs are listed in Table 2.

After the testing samples are obtained, we can use these ground truth ROIs through the confusion matrix function to obtain the total accuracy and kappa coefficient. The accuracy of the classification and the kappa coefficients are shown in Table 3.

The final accuracy indicates that the support vector machine performed well in the supervised classification of 11 TM/OLI/TIRS phases. We can therefore analyze the evolution of the Pearl River Delta from its temporal and spatial changes.

3.1 Temporal variations

Through the statistics of the area with different objects in each TM/OLI/TIRS image, the temporal variation of different region classifications is shown in Fig. 4.

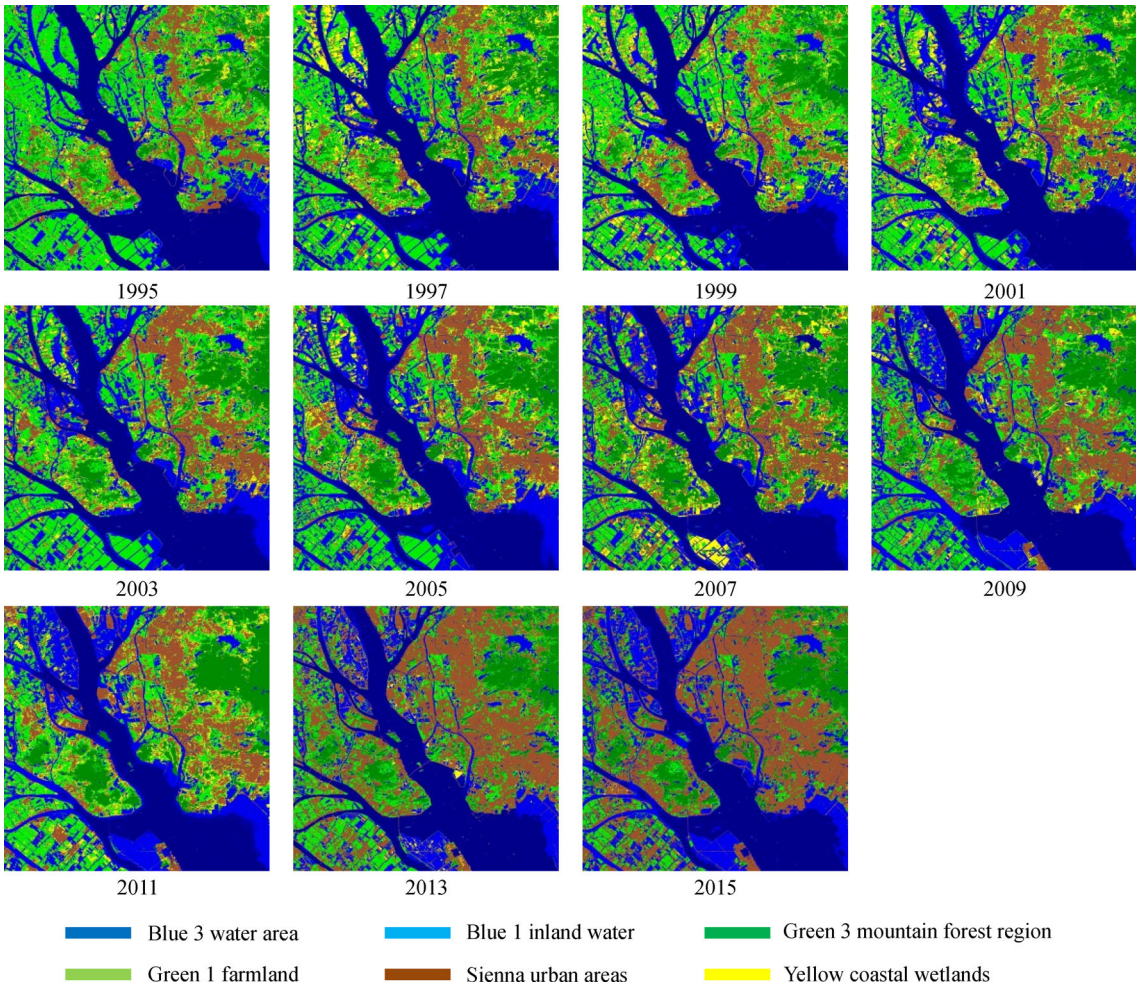

Fig. 3 Output images using the SVM classification on the original images shown in Fig. 2.

Table 2 Statistics listing the number of testing samples used

Year	Water	Mountain forest	Urban areas	Inland water	Coastal wetland	Farmland
1995	812	362	491	432	203	667
1997	868	518	672	823	126	1200
1999	807	330	792	511	215	939
2001	983	766	988	822	123	1229
2003	530	792	603	797	194	716
2005	956	874	844	803	127	658
2007	784	637	1131	768	218	547
2009	1040	742	1025	1226	122	732
2011	746	718	648	510	99	383
2013	923	725	1732	970	86	486
2015	1011	1022	1585	881	108	532

From the result, we can see that the urban area has noticeably increased in the past twenty years, with 2015 showing 1.5 times more growth since 1995. The reason for this increasing trend is mainly because rapid economic growth increases the population in the Pearl River Delta.

From Fig. 5(a), the population in the Pearl River Delta

Table 3 Accuracy of regional classifications in Pearl River Delta for each image used

Year	Total accuracy/%	Kappa coefficient
1995	91.61	0.89
1997	92.24	0.90
1999	97.39	0.97
2001	94.18	0.93
2003	97.37	0.97
2005	97.37	0.97
2007	94.97	0.94
2009	95.91	0.95
2011	96.58	0.96
2013	94.62	0.93
2015	92.08	0.89

was obtained from the Guangdong statistical yearbook[1)]. We can see that the urban population and total population both had a gradually increasing trend in the past twenty years, while over the same time period; the population in the rural area had a decreasing trend.

For other land classifications, both farmland and coastal wetlands have shown a decreasing trend in the past twenty years. We can see that the decline of the farmland is negatively correlated with the increase of urban land use. In Fig. 5(b), we see that the main cause for this phenomenon is the rapid development of the economy, which has made agriculture (primary industry) shrink, and the divergence between the incomes of farmers and non-farmers increase. A likely reason for the decreasing trend of coastal wetlands (intertidal beach and inland swamp) is attributed to anthropogenic activities, yielding substantial damage to the natural environment. Indeed, we can see that the coastal wetland in the Pearl River Delta nearly disappeared in the past twenty years.

Besides the three ROIs discussed above (urban area, farmland, and coastal wetland), the other three land classifiers (inland water, mountain forest, and water) fluctuated throughout the 20 year span of the study, and the final area change was not clearly determined.

The variation of the total wetland area in the Pearl River Delta in the past twenty years is shown in Fig. 5(c); we can see that the wetland gradually decreased from 124,219.5 acres in 1995 to 97,660.1 acres in 2007. In 2007, the wetlands of the Pearl River Delta increased slightly, with about 15,183 acres at the end of 2011. In the last four years of our study period, there was widespread coastal wetland and farmland degradation because of rapid urban expansion.

3.2 Spatial variations

By using the change detection statistics function in ENVI®, we can obtain the transformational matrix for the ROIs we selected on the TM/OLI/TIRS phases, with the final matrix shown in Table 4.

From the matrix, we can see that the areas of water, coastal wetland, and farmland all had decreasing trends, with a loss of 8226.0 (−16.20%), 21,052.3 (−95.58%), and 32,751.2 (−54.89%) acres between the initial year 1995 and the final year 2015. On the contrary, the areas of mountain forest, urban land, and inland water increased 2861.9 (15.43%), 51078.3 (177.19%), and 8089.2 (19.02%) acres, respectively. Besides the spatial changes of the same type of object seen in the TM/OLI/TIRS images, the transformational matrix can also reflect the spatial changes between different ROIs. For the urban land, which showed the most growth in the past twenty

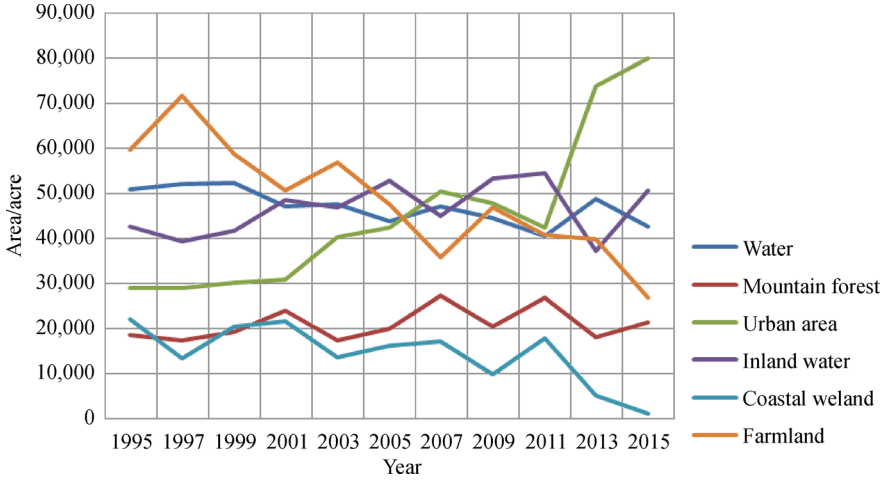

Fig. 4 The change of different land classification regions in the Pearl River Delta from 1995 to 2015.

1) Statistics Bureau of Guangdong Province (1996–2016). Guangdong Statistical Yearbook. Beijing: China Statistical Publishing House.

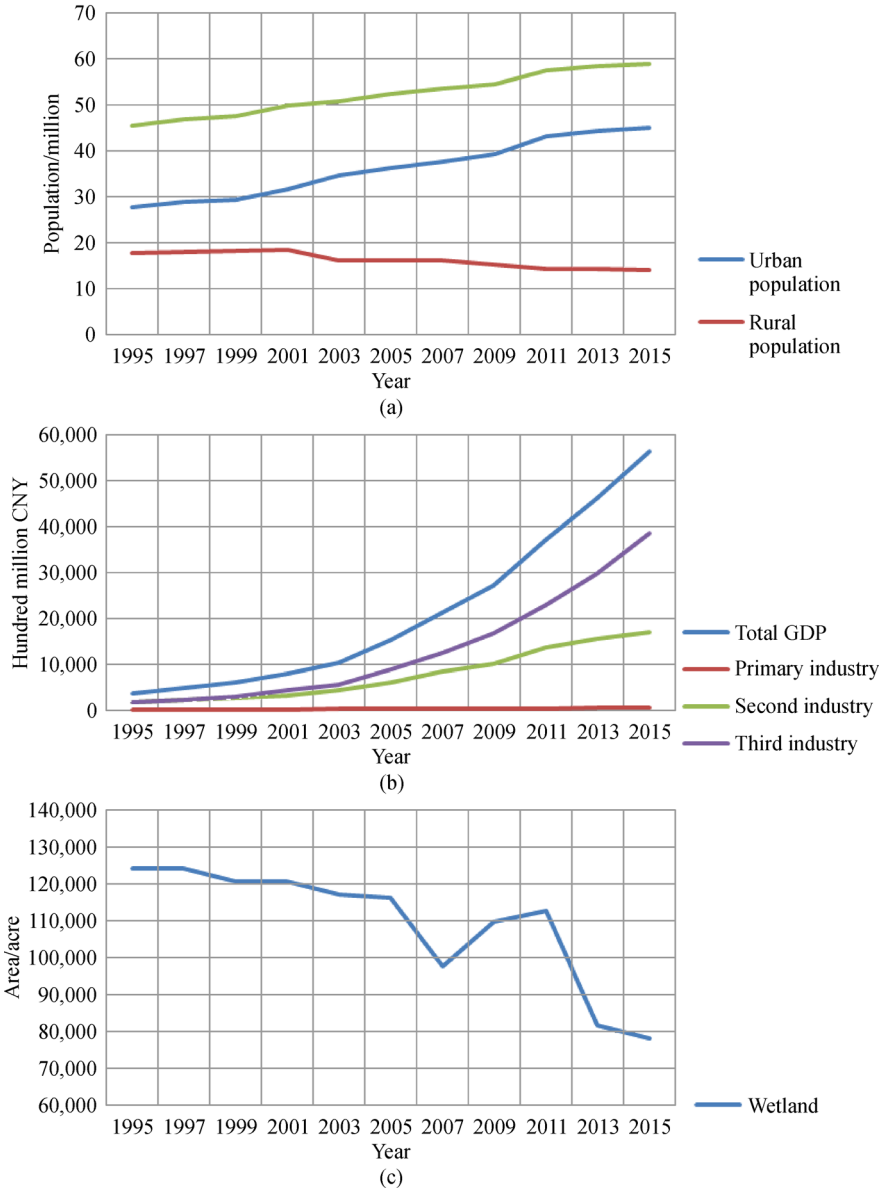

Fig. 5 (a) Population statistics in the Pearl River Delta from 1995 to 2015, showing changes in urban and rural populations, as well as total population. (b) GDP statistics in the Pearl River Delta from 1995 to 2015, (c) The total change of wetland areas in the Pearl River Delta from 1995 to 2015.

years, it can be seen that farmland area had changed by 28,155.7 (47.19%) acres to urban areas; that coastal wetlands changed 12,581.7 (57.12%) acres to construction areas, and that inland water regions lost approximately 12,152.5 (28.57%) acres, which is nearly the same as the coastal wetland for urban expansion. The first three land use regions are all wetlands, which means that urban expansion is the most likely cause of the descending trend of wetland extent in the Pearl River Delta. Farmland lost the most area among the six land covers. From the table, it can be seen that 47.19% of farmland areas (about 28,155.7 acres) is now occupied by urban areas, and the largest gained areas from the farmland were: inland water (approximately 10,564.6 acres) and mountain forest (about 6295.4 acres). Although the farmland lost the most total area, the reduction of the coastal wetland area was the highest by percentage. Almost 95.58% of the coastal wetland has been changed to other land uses in the past twenty years, primarily to construction activities (57.12%), inland water (19.39%), and farmland (17.47%).

4 Discussion

In this study, we used the TM image in 1995 as experimental data to compare the support vector machine

Table 4 The transformational matrix for different region classifications in the Pearl River Delta between 1995 and 2015 (unit: acre)

Final state	Initial state					
	Water	Mountain forest	Urban area	Inland water	Coastal wetland	Farmland
Water	40,839.3 (80.41%)	2.9 (0.02%)	5.3 (0.02%)	1653.0 (3.89%)	6.0 (0.03%)	58.7 (0.10%)
Mountain forest	9.6 (0.02%)	12,185.2 (65.68%)	703.6 (2.44%)	1019.0 (2.40%)	1201.8 (5.46%)	6295.4 (10.55%)
Urban area	866.9 (1.71%)	3461.5 (18.66%)	22,687.6 (78.70%)	12,152.5 (28.57%)	12,581.7 (57.12%)	28,155.7 (47.19%)
Inland water	9009.7 (17.74%)	843.3 (4.55%)	2556.4 (8.87%)	23,373.4 (54.96%)	4271.4 (19.39%)	10,564.6 (17.71%)
Coastal wetland	17.8 (0.04%)	72.7 (0.39%)	87.0 (0.30%)	266.0 (0.63%)	116.3 (0.53%)	413.6 (0.69%)
Farmland	48.0 (0.10%)	1987.1 (10.71%)	2787.7 (9.67%)	4065.7 (9.56%)	3848.5 (17.47%)	14,176.0 (23.76%)
Class changes	9952.0 (19.59%)	6367.5 (34.32%)	6140.0 (21.30%)	19,165.2 (45.04%)	21,909.4 (99.47%)	45,488.1 (76.24%)
Image Difference	−8226.0 (−16.20%)	2861.9 (15.43%)	51,078.3 (177.19%)	8089.2 (19.02%)	−21,052.3 (−95.58%)	−32,751.2 (−54.89%)

(SVM) method with other conventional methods, such as the unsupervised classification (IsoData) or the supervised classification (Maximum Likelihood and Minimum Distance).

4.1 SVM versus IsoData

By using the SVM and IsoData methods, the classified images of the study area in 1995 are shown in Fig. 6(a).

From the two output images, we can see that the SVM (left panel) has a better result than the IsoData (right panel). For example, the inland water in our study was clearly classified by SVM method, but the IsoData method mixed it with sea water. Also, the mountain forest cannot be separated from the farmland in the right image, which causes incorrect classification of the wetland in the Pearl River Delta. In addition, we can also use the confusion matrix method to evaluate the accuracy of IsoData method. In Table 5, it can be seen that the final accuracy of the IsoData classification methods is lower than that of SVM method in our study area.

4.2 SVM versus minimum distance

The minimum distance technique uses the mean vectors of each end member and calculates the Euclidean distance from each unknown pixel to the mean vector for each class. All pixels are classified into the nearest class unless a standard deviation or distance threshold is specified, in which some pixels may be unclassified if they do not meet the selected criteria. The final result of this method is shown in Fig. 6(b).

From the final result, we can see that the minimum distance method confused the urban areas with other objects on the ground, especially the mountain forest. Meanwhile, the inland water, such as some known freshwater reservoirs, was mixed with the sea water in the minimum distance method. The final accuracy result in Table 5 showed that the Minimum Distance method was not a good classification template to extract wetland regions from the TM/OLI/TIRS images in the Pearl River Delta.

4.3 SVM versus maximum likelihood

The maximum likelihood method assumes that each band of statistical class is in a normal distribution, and then calculates the likelihood of a given pixel that belongs to a training sample. The pixel is eventually merged into the maximum likelihood of the class. The classification results of maximum likelihood method and SVM are in Fig. 6(c).

In the analysis of this group, we can see the output image of the Maximum Likelihood method properly discriminates the inland water from the sea water. Also, the coastal wetland is separated from the urban area with a relatively high accuracy. However, the classification between mountain forest and farmland is not satisfactory, especially in the area of Dongguan City on the upper right of our study area. Similar to the other comparisons, the accuracy comparison between these two methods is given in Table 5. From the table we can see the accuracy and kappa coefficient of Maximum Likelihood method was better than the IsoData method and Minimum Distance method, but obviously lower than the SVM method.

5 Conclusions

In this study, 11 images of TM/OLI/TIRS are tested for wetland classification in the Pearl River Delta by using

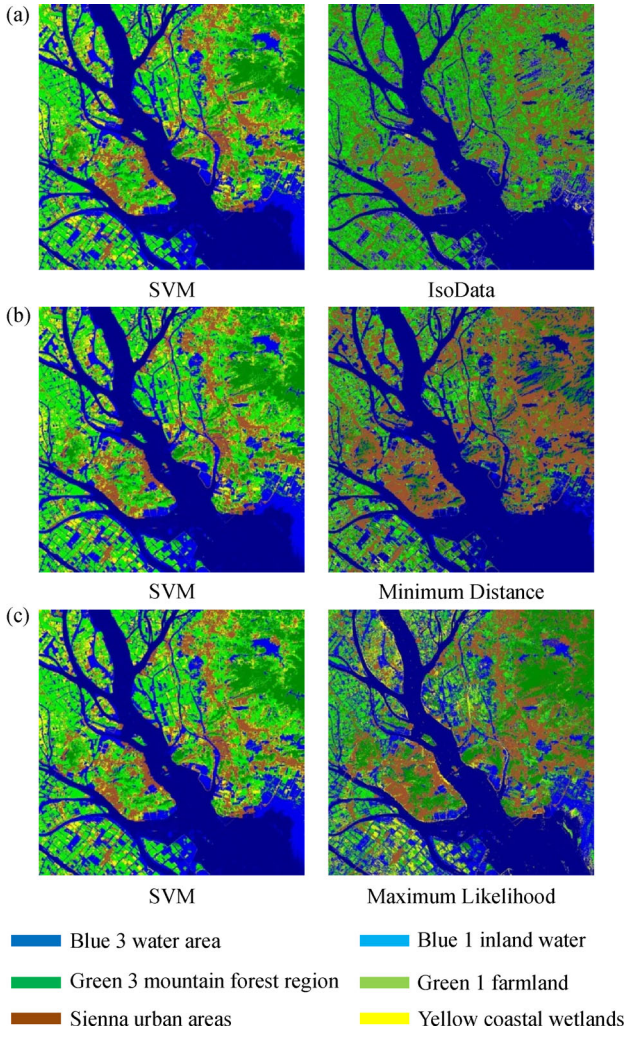

Fig. 6 Comparisons of the SVM method to other methodologies: (a) Comparisons between SVM and IsoData (1995), (b) Comparisons between SVM and Minimum Distance (1995), (c) Comparisons between SVM and Maximum Likelihood (1995).

Table 5 Accuracy comparisons between SVM and IsoData, minimum distance and maximum likelihood methods

Item	The total accuracy/%	Kappa coefficient
SVM	91.61	0.89
IsoData	59.08	0.49
Minimum distance	60.03	0.50
Maximum likelihood	77.69	0.73

SVM combined with field data. The total classification resolution reaches 94.94% and the kappa coefficient exceeds 0.94. Compared with other classification methods, SVM shows the best classification accuracy in the wetland investigation. Based on the SVM clarification results, the wetland area in our research area had decreased by 45,875.6 acres over the past twenty years, suggesting that excessive and rapid urbanization was a main reason for wetland degradation.

Wetlands in coastal areas have complicated and mixed spectral characteristics and dynamic properties that are different from those of inland areas. For a test area of the Pearl River Delta, this study shows that the SVM method can be successfully used to identify the wetland area from satellite images with very high accuracy, and suggests that the SVM is a practical method for the satellite image-based coastal zone classification. The results will be helpful for the survey of large area of wetland in other areas.

Acknowledgements This work is supported by the General Research Fund of Hong Kong Research Grants Council (RGC) under Grants CUHK 402912 and 403113, the Hong Kong Innovation and Technology Fund under Grant ITS/321/13, the direct grants of the Chinese University of Hong Kong, and the National Natural Science Foundation of China (Grant Nos. 41376035, 41376125, and 41006070).

References

Brennan R L, Prediger D J (1981). Coefficient kappa: some uses, misuses, alternative. Educ Psychol Meas, 41(3): 687–699

Ceamanos X, Waske B, Benediktsson J A, Chanussot J, Fauvel M, Sveinsson R (2010). A classifier ensemble based on fusion of support vector machines for classifying hyperspectral data. Int J Image Data Fusion, 1(4): 293–307

Cohen J (1960). A coefficient agreement for nominal data. Educ Psychol Meas, 20(1): 37–46

Dahl T (2006). Status and Trends of Wetlands in the Conterminous United States 1998 to 2004. Fish and Wildlife Service Publication, 1–112

Fan H G, Yue C E, Wang D (2014). Remote sensing classification and land cover change in Yi Liang County based on support vector machine Method. Forest Inventory and Planning, 39(2): 51–56 (in Chinese)

Kamlun K U, Bürger Arndt R, Phua M H (2016). Monitoring deforestation in Malaysia between 1985 and 2013: insight from South-Western Sabah and its protected peat swamp area. Land Use Policy, 57: 418–430

Kristine Butera M (1983). Remote sensing of wetlands. IEEE Trans Geosci Remote Sens, GE-21(3): 383–392

Li L K (2001). Wetland and ramsar convention. World Forestry Research, 14: 1–7

Liang S L, Fang H L, Chen M Z (2001). Atmospheric correction of Landsat ETM + land surface imagery—Part I: methods. IEEE Trans Geosci Remote Sens, 39(11): 2490–2498

Lillesan T M, Kiefer R W (2000). Remote Sensing and Image interpretation (4th ed). Hoboken: John and Sons Inc.

Lin Y, Shen M, Liu B, Ye Q (2013). Remote sensing classification method of wetland based on an improved SVM. ISPRS-International Archives of the Photogrammetry, Remote Sensing and Spatial Information Sciences, XL-7(W1): 179–189

Melgani F, Bruzzone L (2004). Classification of hyperspectral remote sensing images with support vector machines. IEEE Trans Geosci

Remote Sens, 42(8): 1778–1790

Næsset E (1996). Use of the weighted Kappa coefficient in classification error assessment of thematic maps. Int J Geogr Inf Syst, 10(5): 591–603

Niu Z G, Zhang H Y, Wang X W, Yao W B, Zhou D M (2012). Mapping wetland changes in China between 1978 and 2008. Chinese Science Bulletin, 57(16): 1400–1411

Powers D M W (2011). Evaluation: from precision, recall and f-measure to ROC, informedness, markedness & correlation. Journal of Machine Learning Technologies, 2(1): 37–63

Pretorius L, Brown L R, Bredenkamp G J, van Huyssteen C W (2016). The ecology and classification of wetland vegetation in the Maputaland Coastal Plain, South Africa. Phytocoenologia, 46(2): 125–139

Silva J P, Phillips L, Jones W, Eldridge J, O'Hara E (2007). LIFE and Europe's Wetlands. Luxembourg: Office for Official Publications of the European Communities

Stehman S V (1997). Selecting and interpreting measures of thematic classification accuracy. Remote Sens Environ, 62(1): 77–89

Vapnik V N (1995). The Nature of Statistical Learning Theory. New York: Springer-Verlag

Wang S G, Li X, Liu K, Zhou Y Z (2007). Dynamic analysis of the wetland resource changes in the estuary of the Pearl River Delta using remote sensing. Acta Scientiarum Naturalium Universitatis Sunyatseni, 46(2): 105–109 (in Chinese)

Waske B, Benediktsson J A (2007). Fusion of support vector machines for classification of multisensor data. IEEE Trans Geosci Remote Sens, 45(12): 3858–3866

Wu W T, Zhou Y X, Tian B (2017). Coastal wetlands facing climate change and anthropogenic activities: a remote sensing analysis and modelling application. Ocean Coast Manage, 138: 1–10

Wu X M, Zhang H Q, Lin H, Liu P P (2012). Study on the prediction of wetland change in Beijing based on support vector machine. Chinese Agricultural Science Bulletin, 28(14): 280–284 (in Chinese)

Zhang C, Wang T, Atkinson P M, Pan X, Li H (2015). A novel multi-parameter support vector machine for image classification. Int J Remote Sens, 36(7): 1890–1906

Zhao Y S (2003). Principles and Methods of Remote Sensing Application Analysis. Beijing: Science Press, 241–249